***SUPPLEMENTARY Table 1**: Thermodynamic Parameters of the interaction between Rb and cellular E2F2 and E1A peptides and proteins.*

	ITC [2]					Fluorescence Spectroscopy			
						Direct titration [3]		Competition [4]	
Titrant [1]	**n**	***ΔH*** (cal/mol)	***-TΔS*** (cal/mol)	***ΔG*** (cal/mol)	K_D (nM)	***ΔG*** (cal/mol)	K_D (nM)	K_D (nM)	**IC50** (nM)
E2F2	0.94 ± 0.01	-8646 ± 174	-2170 ± 302	-10817 ± 247	8.7 ± 3.6	-12057 ± 16	1.03 ± 0.03	4.7 ± 0.3	30
E1A$_{E2F}$[5]	0.73 ± 0.06	1100 ± 144	-9102 ± 469	-8003 ± 446	1080 ± 828	-9286 ± 10	119.1 ± 2.1	299 ± 45	2000
E1A$_{LxCxE}$	1.03 ± 0.01	-9522 ± 79	573 ± 92	-8949 ± 47	213 ± 17	-9362 ± 16	104.6 ± 2.9	-	-
E1A$_{LxCxE\text{-}AC}$	1.02 ± 0.01	-10127 ±122	511 ± 161	-9615 ± 104	68.5 ± 12.3	-9577 ± 18	73.4 ± 2.2	*nd*	*nd*
E1A$_{LxCxE\text{-}ACP}$	1.19 ± 0.01	-7900 ± 107	-2021 ± 168	-9921 ± 129	40.6 ± 9.1	-10339 ± 16	19.6 ± 0.5	*nd*	*nd*
E1A$_{WT}$[6]	1.19 ± 0.01	-5284 ± 40	-8960 ± 105 [a]	*nd*	*nd*	-14244 ± 97	0.024 ± 0.004	0.065 ± 0.009	1.5
E1A$_{\Delta E}$	0.92 ± 0.01	-10784 ± 95	452 ± 140	-10332 ± 103	19.9 ± 3.8	-9828 ± 21	47.1 ± 1.7	*nd*	*nd*
E1A$_{\Delta L}$[5]	0.92 ± 0.05	2447 ± 291	-10553 ± 477	-8106 ± 378	904 ± 578	-8966 ± 9	206.7 ± 3.1	248 ± 37	1500

Most measurements were performed in triplicate except for the ITC titrations for Rb-E1A$_{WT}$ which was performed in duplicate and for Rb-E1A$_{E2F}$ which was performed once. For competition experiments, titrations were performed at least twice but values are from a single experimental set.

[1] All ITC and Fluorescence Spectroscopy measurements were performed at 20.0 °C.

[2] For ITC experiments, n values are the average of all independent experimental determinations and the standard deviation is obtained as the propagated mean standard error. ΔH and K_D values are the average of all independent experimental determinations. The standard deviations for ΔH and K_D are obtained as propagated mean standard errors. ΔG is calculated as $\Delta G = RT*LnK_D$ and $-T\Delta S$ as $-T\Delta S = \Delta G - \Delta H$. The standard deviations for ΔG and $-T\Delta S$ are obtained as the propagated mean standard errors.

[3] For Fluorescence Spectroscopy direct titration experiments, the K_D value was obtained from a global fitting of three independent experimental determinations performed at different protein concentrations (**See Methods**). The error for K_D is the standard error of the fitted parameter. ΔG is calculated as $\Delta G = RT*LnK_D$ and its standard deviation is obtained by error propagation.

[4] For Fluorescence Spectroscopy competition experiments, the error for K_D is the standard error of the fitted parameter.

[5] The discrepancy in the K_D values obtained by ITC versus fluorescence spectroscopy for these two variants is likely to be due to slow kinetics of binding that leads to an underestimation of the binding affinity in the ITC experiments.

[6] In previous studies of E1A binding to Rb the Cys residue in the LxCxE motif was mutated to Ala, which reduced the affinity of the complex to K_D ~ 4 nM [[1]].

[a] Calculated using ΔG from Fluorescence data

Values for thermodynamic parameters are: R = 1.985 cal/K*mol. T = 283.15 K (10 ºC) or T = 293.15 K (20 ºC).

- No value could be fitted to the displacement curve as it had no change in fluorescence over the concentration range tested.

nd: not determined

***SUPPLEMENTARY Table 2**: Analysis of quaternary structure and hydrodynamic behavior of unbound Rb and E1A proteins and [Rb:E1A] complexes.*

	MW_{THEO} [1] (kDa)	MW_{SLS} [2] (kDa)	MW_{SLS} [3] /MW_{THEO}	$MW_{app\ SEC}$ [4] /MW_{THEO}	R_h (nm) [5] EXPERIMENTAL	R_h (nm) [6] ENSEMBLE 25ºC	R_h (nm) [7] ENSEMBLE 20ºC	R_g (nm) [8] SAXS	R_g /R_h [9]	**v** [10]
E1A$_{WT}$	12.5	13.93	1.11	4.35 4.77 ± 0.01 [a]	3.07 ± 0.12 3.42 ± 0.01 [b]	-	-	4.28 ± 0.02 4.64 ± 0.03 4.51 ± 0.02	1.39 1.25 [d]	0.64 [e] 0.53 [f] 0.55 [g]
E1A$_{\Delta L}$	12.2	11.58	0.95	4.40	3.03 ± 0.12	-	-	-	-	-
E1A$_{\Delta E}$	12.1	12.96	1.07	4.36	3.07 ± 0.12	-	-	-	-	-
Rb	42.1	38.82	0.92	1.09	2.94 ± 0.12	-	-	2.42 ± 0.02 2.50 ± 0.01 2.61 ± 0.01	0.82	0.38 [f]
[Rb:E1A$_{WT}$]	54.6	56.3	1.03	1.12	3.20 ± 0.12	3.27 3.36 [c]	3.71 3.79 [c]	2.98 ± 0.04 2.97 ± 0.02 3.33 ± 0.02	0.93	-
[Rb:E1A$_{\Delta E}$]	54.2	53.9	0.99	1.20	3.34 ± 0.13	3.64	4.12	-	-	-
[Rb:E1A$_{\Delta L}$]	54.3	56.2	1.03	1.27	3.27 ± 0.12	3.60	4.07	-	-	-

[1] MW_{THEO} is the theoretical monomeric molecular weight of each free protein and for the complexes it results from the sum of their molecular weights considering a 1:1 complex.
[2] MW_{SLS} was experimentally determined by SEC-SLS at RT.
[3] MW_{SLS}/MW_{THEO} ratios indicate the oligomerization state of unbound proteins and stoichiometry for the protein complexes. Value 1 indicates a monomer state for unbound proteins and a [1:1] stoichiometry for complexes.
[4] MW_{appSEC}/MW_{THEO} ratios indicate the extended or compact hydrodynamic behavior of the unbound proteins and complexes. MW_{appSEC} corresponds to the molecular weight estimated from the calibration curve in SEC experiments (**See Methods**). Values above 1 indicate an extended behavior.
[5] $R_{h\ EXPERIMENTAL}$ was calculated from SEC data as: log R_h = -0.204 + 0.357 log MW_{appSEC} [2] and its standard deviation was obtained by error propagation.
[6,7] $R_{h\ ENSEMBLE}$ was calculated for generated ensembles at 25 ºC and 20 ºC respectively using the program HydroPro as explained in (**See Methods**) or from the sub-ensembles selected by EOM. The SEC results showed that [Rb:E1A$_{\Delta L}$] and [Rb:E1A$_{\Delta E}$] were more expanded than [Rb:E1A$_{WT}$], as expected from a single motif being bound to Rb (**Fig. 3f**). The measured R_h values were lower than those obtained from computed ensembles (**Fig. 3g)**, suggesting that the linker sampled slightly more compact conformations in these mutants.
[8] $R_{g\ SAXS}$ was calculated from SAXS experiments. SAXS measurements were performed at three different concentrations for E1A$_{WT}$, Rb and the [Rb:E1A$_{WT}$] complex (**See Methods**) and for the sake of completeness R_g derived from all concentrations tested are informed. An increase in R_g at 2.7 mg/ml of [Rb:E1A$_{WT}$] complex indicated inter-particle interaction and the Guinier region for this concentration was not used for further analysis.
[9] Ratio of SAXS-derived R_g to experimental R_h (R_g/R_h) for free and bound proteins. The R_g values used here correspond to those calculated from the Guinier region in the final merged SAXS profiles of E1A$_{WT}$, Rb and [Rb:E1A$_{WT}$] complex, which contain information from the lowest concentration data. The R_g/R_h ratio provides a measure of chain compactness. Ratio values of 0.75, 1.0 and 1.50 are expected for compact globules, Flory random chains (FRC) and for excluded volume (EV) chains respectively. For Flory random chains, modest deviations around 1.0 are probably the result of stronger intrachain repulsions or attractions [3] [4]. Unless noted otherwise the R_h values used here are derived from SEC experiments. Combined SAXS and SEC-SLS measurements confirmed that while Rb had a compact conformation (R_g/R_h = 0.82), *E1A$_{WT}$* was highly extended (R_g/R_h = 1.39). In contrast [Rb:E1A$_{WT}$] had an R_g/R_h = 0.93, consistent with compaction upon bivalent tethering.
[10] The exponent *v* was calculated by applying the scaling law $R_x=R_0N^v$ where R_x might be R_h or R_g. and R_0 depends on the dimensions of the chain and was obtained as described in e, f and g. The reference values for v depend on the dimensions of the chain and are 0.6 for an excluded volume chain, 0.33 for a compact globule and 0.5 for a chain in the Θ-regime [4].

[a] Found as MW_{DLS}/MW_{THEO} where MW_{DLS} was obtained from three independent DLS measurements (**See Methods**).
[b] Obtained from three independent DLS measurements.
[c] R_h values corresponding to the sub-ensembles selected by EOM that best fit SAXS data (**Figure 3**).
[d] R_g/R_h for E1A$_{WT}$ using R_h derived from DLS experiments.
[e] v was fitted using R_g obtained from SAXS measurements using the formula $R_g=R_0N^v$ with R_0 = 2.1 nm and N= 114 for E1A$_{WT}$. The R_0 value is from [4].
[f] v was fitted using R_h obtained from SEC-SLS measurements using the formula $R_h=R_0N^v$ with R_0 = 2.49 nm and N= 114 for E1A$_{WT}$ and R_0 = 4.92 nm and N= 360 for Rb. The R_0 values are from [5].
[g] v was fitted using R_h obtained from using DLS measurements using the formula $R_h=R_0N^v$ with R_0 = 2.49 nm and N= 114 for E1A$_{WT}$. The R_0 values are from [5].

***SUPPLEMENTARY Table 3**: Dissociation constants for the interaction between Rb and cellular E2F2 and E1A peptides and proteins*

Probe	(nM)	K_D (nM)	K_D (nM)	r(*0*)	r(*F*)	F(*0*)	F(*F*)
		Raw data	Normalized data				
E2F2	1	1.18 ± 0.16	1.15 ± 0.05	0.062	0.163		
	5	0.91 ± 0.04	0.91 ± 0.02	0.049	0.209		
	10	0.71 ± 0.05	0.74 ± 0.03	0.043	0.219		
	20	1.39 ± 0.16	1.55 ± 0.05	0.043	0.215		
	30	1.06 ± 0.08	1.14 ± 0.05	0.043	0.227		
	K_D global fit		1.03 ± 0.03				
E1A$_{E2F}$	100	109.3 ± 9.7	97.6 ± 3.6	0.046	0.198		
	200	100.2 ± 22.4	97.4 ± 5.6	0.049	0.206		
	300	101.3 ± 11.4	93.2 ± 4.2	0.049	0.206		
	500	105.5 ± 10.2	93.4 ± 4.4	0.050	0.211		
	1000	127.9 ± 12.2	75.1 ± 7.9	0.045	0.203		
	2000	109.5 ± 0.6	81.6 ± 4.9	0.046	0.206		
	K_D global fit		119.1 ± 2.1				
E1A$_{LxCxE}$	100	113.4 ± 14.1	117.2 ± 6.5	0.028	0.076		
	200	93.1 ± 11.3	93.5 ± 2.9	0.036	0.091		
	300	93.7 ± 7.9	93.0 ± 2.6	0.033	0.087		
	500	97.9 ± 15.6	98.7 ± 3.7	0.032	0.088		
	1000	117.1 ± 28.3	111.9 ± 7.4	0.032	0.086		
	K_D global fit		104.6 ± 2.9				
E1A$_{LxCxE\text{-}AC}$	130	80.7 ± 12.8	80.5 ± 6.9	0.04	0.100		
	175	73.7 ± 5.2	73.7 ± 5.2	0.04	0.105		
	700	85.6 ± 7.4	82.8 ± 5.8	0.039	0.106		
	K_D global fit		73.4 ± 2.2				
E1A$_{LxCxE\text{-}ACP}$	30	20.1 ± 2.6	20.1 ± 2.6	0.05	0.099		
	50	20.2 ± 2.4	17.5 ± 1.3	0.04	0.093		
	100	19.5 ± 2.2	18.2 ± 2.2	0.039	0.092		
	K_D global fit		19.6 ± 0.5				
E1A$_{WT}$	0.5	0.025 ± 0.004	0.025 ± 0.003	0.075	0.191		
	0.5	0.027 ± 0.006	0.027 ± 0.003	0.059	0.127		
	0.5	0.026 ± 0.009	0.025 ± 0.008			111.6	98.8
	1	0.037 ± 0.009	0.034 ± 0.005	0.061	0.153		
	1	0.049 ± 0.019	0.050 ± 0.012			302.8	274.9
	2	0.046 ± 0.007	0.047 ± 0.005	0.058	0.143		
	2	0.062 ± 0.008	0.062 ± 0.005	0.064	0.2		
	2	0.065 ± 0.015	0.062 ± 0.009	0.062	0.175		
	2	0.065 ± 0.022	0.092 ± 0.025			773.3	710.1
	2	0.074 ± 0.036	0.090 ± 0.034			412.4	356.1
	2	0.075 ± 0.010	0.074 ± 0.006			613.5	532.6
	K_D global fit		0.024 ± 0.004				
E1A$_{\Delta E}$	50	42.6 ± 3.9	42.5 ± 3.6	0.05	0.105		
	200	53.9 ± 3.1	53.9 ± 3.1	0.05	0.106		
	800	60.2 ± 10.1	54.5 ± 10.3	0.048	0.105		
	K_D global fit		47.1± 1.7				
E1A$_{\Delta L}$	200	197.7 ± 4.5	197.7 ± 4.5	0.058	0.220		
	400	207.5 ± 7.4	207.5 ± 7.4	0.056	0.232		
	800	225.2 ± 20.6	217.9 ± 10.9	0.023	0.219		
	K_D global fit		206.7 ± 3.1				

Fluorescence spectroscopy direct titrations were performed at fixed concentrations of FITC-labeled protein/peptide titrated with increasing amounts of Rb until saturation. For each complex this experiment was performed at different concentrations of FITC-probes. The K_D parameter was obtained from fitting the titration curves to a bimolecular association model from individual titrations using raw and normalized titration curves or by global fitting of the normalized data. An excellent agreement between individual and global fits was obtained. Initial anisotropy signals *r(0)*, showed that intrinsic anisotropy of the FITC-probes are constant and independent of the concentrations tested. Final anisotropy signals *r(F)* reached stable values for the complex with Rb. Initial and final fluorescence signals (*F(0) y F(F)*) were measured only for E1A$_{WT}$ and even though these values represent a more variable range, they proved to be equally useful for fitting K_D values.

***SUPPLEMENTARY Table 4**: Affinity of MBP-E1A constructs representing grafted linkers and endogenous sequences.*

Construct Name	Host [#]	Linker Length	K_D (M) *	*Ratio* [1] *Exp* $K_D/K_{D,E1AWT}$	*Ratio* [2] Lp_{Sim} $K_D/K_{D,E1AWT}$	*Ratio* [3] Lp_3 $K_D/K_{D,E1AWT}$	*Ratio* [4] *Endogenous* $K_{D,ED}/K_{D,E1AWT}$
E2F2	--	--	$2.3 \pm 0.4\ 10^{-9}$	--	--	--	
E1A$_{WT}$(HAdV5)	Human	71	$76 \pm 15\ 10^{-12}$	--	--	--	
MBP-E1A$_{WT}$(HAdV5)	Human	71	$75 \pm 17\ 10^{-12}$	1	1	1	1
MBP-E1A OA$_{BAdV2}$ (Bov-1)	Bovine/Ovine	27	$1.53 \pm 0.05\ 10^{-9}$	20.4 ± 4.7	1.4	14.3	
MBP-E1A OA$_{BAdV2\text{-}ED}$ (Bov-1-ED)	Bovine/Ovine	27	$>1.66 \pm 0.36\ 10^{-6}$	$(2.2 \pm 0.7)\ 10^{4}$	--	--	$4.7\ 10^{6}$
MBP-E1A BA$_{BAdV1}$ (Bov-2)	Bovine/Ovine	28	$9.75 \pm 2.21\ 10^{-9}$	13 ± 4	1.2	11.1	
MBP-E1A HG$_{HAdV52}$ (Hum-1)	Human	41	$87 \pm 9\ 10^{-12}$	1.2 ± 0.3	0.93	2.4	
MBP-E1A HF$_{HAdV40}$ (Hum-2)	Human	48	$30 \pm 9\ 10^{-12}$	0.4 ± 0.2	1.04	1.64	
MBP-E1A SA$_{SAdV3}$ (Sim-1)	Simian	52	$43 \pm 13\ 10^{-12}$	0.6 ± 0.2	0.95	1.4	
MBP-E1A CA$_{CAdV1}$ (Can)	Canine	56	$433 \pm 64\ 10^{-12}$	5.8 ± 1.6	0.95	1.3	
MBP-E1A BtB$_{BtAdV2}$ (Bat)	Bat	57	$360 \pm 70\ 10^{-12}$	4.8 ± 1.4	0.97	1.25	
MBP-E1A BtB$_{BtAdV2\text{-}ED}$ (Bat-ED)	Bat	57	$112 \pm 30\ 10^{-12}$	1.5 ± 0.5	--	--	$1\ 10^{-3}$
MBP-E1A SA$_{SAdV22}$ (Sim-2)	Simian	61	$67 \pm 8\ 10^{-12}$	0.9 ± 0.2	0.97	1.15	
MBP-E1A HC$_{HAdV5}$ (E1A$_{WT}$*ΔHyd*)	Human	71	$50 \pm 6\ 10^{-12}$	0.7 ± 0.2	--	1	
MBP-E1A HA$_{HAdV18}$ (Hum-3)	Human	75	$49 \pm 7\ 10^{-12}$	0.7 ± 0.2	1.11	0.96	
MBP-E1A HF$_{HAdV40\text{-}2x}$ (Hum-2- 2x)	Human	96	$80 \pm 22\ 10^{-12}$	1.1 ± 0.4	--	--	

[#] The column represents the host species infected by each Adenovirus species.

* K_D values are the average of three to five independent titrations, except for the E2F2 and E1A$_{WT}$ complexes, where two titrations were performed.

[1] Ratio of each measured K_D value of the variant to the K_D value of the MBP-E1A$_{WT}$ variant

[2] Ratio of the predicted K_D value of the variant to the predicted K_D value of MBP-E1A$_{WT}$ under the WLC L_{pSim} assumption. K_D values were calculated using the affinity of the E1A$_{WT}$ E2F and LxCxE motifs (reported in **Supplementary Data Table 1**) and the C_{eff} value obtained from the WLC model using sequence dependent L_p values derived from the all-atom simulations (reported in **Source Data for Extended Data Fig. 10**)

[3] Ratio of the predicted K_D value of the variant to the predicted K_D value of MBP-E1A$_{WT}$ under the WLC assumption with a sequence-independent L_p parameter. K_D values were calculated using the affinity of the E1A$_{WT}$ E2F and LxCxE motifs (reported in **Supplementary Data Table 1**) and the C_{eff} value derived from the WLC model using a L_p value of 3.

[4] Ratio of the K_D value for the Endogenous variant to the predicted K_D value of MBP-E1A$_{WT}$ under the WLC assumption with a sequence-independent L_p parameter. For Bov-1 and Bat we used the affinity of the endogenous E2F and LxCxE motifs predicted by FoldX (**Source Data for Extended Data Fig. 10**) and the C_{eff} value derived from the WLC model using a L_p value of 3.

***SUPPLEMENTARY Table 5**: Temperature dependence of thermodynamic parameters and calculation of $_{\Delta}Cp$ values from calorimetric data for the interactions between Rb and* E1A$_{\Delta L}$ or E1A$_{E2F}$.

Titrant	°C	n [1]	ΔH (cal/mol)	$-T\Delta S$ (cal/mol)	ΔG (cal/mol)	K_D (nM)	ΔCp [2] (cal/mol K)
E1A$_{\Delta L}$	10	0.91 ± 0.03	8675 ± 599	-16196 ± 622	-7521 ± 166	1590 ± 487	
E1A$_{\Delta L}$	20	0.92 ± 0.05	2447 ± 291	-10553 ± 477	-8106 ± 378	904 ± 578	-606.3 ± 9.6
E1A$_{\Delta L}$	30	0.94 ± 0.03	-3450 ± 225	-4920 ± 310	-8379 ± 213	922 ± 326	
E1A$_{E2F}$	10	0.86 ± 0.02	7205 ± 338	-14739 ± 364	-7534 ± 134	1535 ± 391	
E1A$_{E2F}$	15	0.86 ± 0.01	4130 ± 122	-11935 ± 156	-7806 ± 98	1200 ± 205	-629.4 ± 7.3
E1A$_{E2F}$	20	0.73 ± 0.06	1100 ± 144	-9102 ± 469	-8003 ± 446	1080 ± 828	
E1A$_{E2F}$	30	0.85 ± 0.02	-5380 ± 246	-2960 ± 301	-8341 ± 173	969 ± 279	

The ΔH and K_D values are the average of all independent experimental determinations. The errors for ΔH and K_D are obtained as propagated mean standard errors. ΔG is calculated as $\Delta G = RT*LnK_D$ and $-T\Delta S$ as $-T\Delta S = \Delta G - \Delta H$. The errors for ΔG and $-T\Delta S$ are obtained as the propagated mean standard errors.
Values for thermodynamic parameters are: R = 1.985 cal/K*mol. T = 283.15 K (10 ºC), T = 288.15 K (15 ºC), T= 293.15 K (20 ºC) and T = 303.15 K (30 ºC).
[1] n values are the average of all independent experimental determinations, and the standard deviation is obtained as the propagated mean standard error.
[2] ΔC_p was calculated from the slope of the ΔH *versus* T curve (**Extended Data Figure 5**)

***SUPPLEMENTARY Table 6**: Calculation of ΔASA_T and X_{res} parameters from calorimetric data for the interactions between Rb and* $E1A_{\Delta L}$ or $E1A_{E2F}$.

Titrant	ΔASA_T [1] (Å²)	ΔASA_T [2] (Å²)	ΔASA_T [3] (Å²)	ΔASA_T [4] (Å²)	ΔASA_T [5] (Å²)	ΔASA_T [6] (Å²)	X_{res} [7]	X_{res} [8]	X_{res} [9]
$E1A_{\Delta L}$	-1945 ± 56	-2848 ± 72	-1676 ± 50	-3793 ± 91	-2564 ± 67	-2755 ± 71	28 ± 1	22 ± 1	33 ± 1
$E1A_{E2F}$	-2120 ± 47	-3035 ± 62	-1828 ± 42	-3951 ± 79	-2748 ± 57	-2949 ± 61	31± 1	25 ± 1	36 ± 1

Structural parameters derived from calorimetry were calculated from [6] as follows*: $\Delta ASA_{total} = \Delta ASA_p + \Delta ASA_{np}$*. First, $\Delta H_{int(TH)}$ was calculated by solving the equation: $\Delta H_{int(T°C)} = \Delta H_{int(TH)} + \Delta C_p(T-T_H)$; where $\Delta H_{int(T°C)}$ is the experimental enthalpy value at working temperatures (T= 283.15, 288.15, 293.15 o 303.15 K), ΔC_p is the change in heat capacity, and T_H is the enthalpic convergence temperature (295.15 K) [7,8]. Second, ΔASA_{total} was calculated by solving the set of equations: $\Delta H_{int(TH)} = \Delta h_{np}\,\Delta ASA_{np} + \Delta h_p\,\Delta ASA_p$ and $\Delta C_p = \Delta c_{np}\,\Delta ASA_{np} + \Delta c_p\,\Delta ASA_p$. Fixed values were used for Δh_{np}= -8.43 cal(molÅ²)$^{-1}$ and Δh_p= 31.29 cal(molÅ²)$^{-1}$. For each set of calculations, the Δc_{np} and Δc_p values were varied as indicated. Our estimates from ITC vary according to the coefficients for hydration heat capacity of polar and nonpolar protein surfaces used [9], which make this calculation a bit controversial:

[1] Parameters derived from Murphy & Freire [10]: Δc_{np} =0.45 cal K^{-1}(molÅ²)$^{-1}$; Δc_p = -0.26 cal K^{-1}(molÅ²)$^{-1}$

[2] Parameters derived from Myers [11]: Δc_{np} =0.29 cal K^{-1}(molÅ²)$^{-1}$; Δc_p = -0.095 cal K^{-1}(molÅ²)$^{-1}$

[3] Parameters derived from Makhatadze & Privalov [12]: Δc_{np} =0.5 cal K^{-1}(molÅ²)$^{-1}$; Δc_p = -0.22 cal K^{-1}(molÅ²)$^{-1}$

[4] Parameters derived from Robertson & Murphy [13]: Δc_{np} =0.17 cal K^{-1}(molÅ²)$^{-1}$; Δc_p = 0.12 cal K^{-1}(molÅ²)$^{-1}$

[5] Parameters derived from Theisen *et al* [9]: Δc_{np} =0.33 cal K^{-1}(molÅ²)$^{-1}$ and Δc_p = -0.14 cal K^{-1}(molÅ²)$^{-1}$

[6] or Spolar & Record [14]: Δc_{np} =0.31 cal K^{-1}(molÅ²)$^{-1}$ and Δc_p = -0.14 cal K^{-1}(molÅ²)$^{-1}$

Differences in ΔASA_{total} between $E1A_{E2F}$ and $E1A_{\Delta L}$ are lower than 10% in all cases independently of the parameters used for their calculation, supporting the conclusion that there is no significant contribution of the linker region to the interaction with Rb.

The values for ΔASA_{total} for $E1A_{E2F}$ derived from ITC are slightly larger than the interaction surface calculated from the crystal structure of the [Rb:$E1A_{E2F}$] complex: ΔASA_{total} = 1623 Å² (PDB 2R7G [15]), indicating that the interaction surface in solution likely involves additional residues to those solved in the X-Ray structure.

X_{res} represents the number of residues involved in folding upon binding in a protein-ligand interaction and was calculated from: $X_{res} = \Delta S_{config}/\Delta S_{residue}$, where ΔS_{config} represents the total change in conformational entropy and $\Delta S_{residue}$ is the reference value for the entropy loss upon folding of one residue. The change in conformational entropy was calculated as $\Delta S_{config} = \Delta S_{rt} - \Delta S_{solv}$ with $\Delta S_{solv} = C_1{*}\Delta C_p{*} \ln (T/T_S)$, where ΔS_{rt} and ΔS_{solv} are the changes in rotation-translation entropy and solvation entropy respectively, T is the experimental temperature (T= 308.15 K, for $E1A_{E2F}$ and 311.65 K for $E1A_{\Delta L}$) and T_S is the temperature for entropic convergence (385K) [7,8]. The calculations assumed different values for ΔS_{rt}, $\Delta S_{residue}$ and the constant C_1, which depends on the relationship of apolar to polar surface area:

[7] Parameters from Perozzo *et. al*.[6] : ΔS_{rt}= -8 cal/K mol, $\Delta S_{residue}$ = -4.3 cal/K mol and C_1= 1

[8] Parameters derived from Spolar & Record [14]: ΔS_{rt}= -50.2 cal/K mol, $\Delta S_{residue}$ = -5.7 cal/K mol and C_1= 1.35

[9] Parameters derived from Thiesen *et. al*.[9]: ΔS_{rt}= -27 cal/K mol, $\Delta S_{residue}$ = -5.7 cal/K mol and C_1= 1.66.

Based on $E1A_{E2F\ (37\text{-}51)}$ being 16-residues long, the remaining residues involved in this interaction should be provided by Rb. Using a criterion of 4Å separation between residues (as upper limit for non-covalent interactions), a structural analysis of PDB 2R7G using PyMOL yielded 32 residues (23 from Rb and 9 from $E1A_{E2F\ (37\text{-}49)}$) involved in the interaction, in close agreement with our estimates from ITC.

***SUPPLEMENTARY Table 7**: Analysis of the allosteric effect between E1A binding sites.*

Cell	Titrant [1]	n [2]	ΔH (cal/mol)	$-T\Delta S$ (cal/mol)	ΔG (cal/mol)	K_D (nM)	$\Delta\Delta G$ [3] (cal/mol)
Rb	**E1A$_{E2F}$**	0.86 ± 0.02	7205 ± 338	-14739 ± 364	-7534 ± 134	1535 ± 392	
Rb + E1A$_{LxCxE}$	**E1A$_{E2F}$**	0.89 ± 0.01	6875 ± 214	-14510 ± 236	-7634 ± 99	1327 ± 159	-100 ± 166
Rb	**E1A$_{\Delta L}$**	0.91 ± 0.03	8675 ± 599	-16196 ± 622	-7521 ± 166	1590 ± 487	
Rb + E1A$_{LxCxE}$	**E1A$_{\Delta L}$**	0.86 ± 0.02	6795 ± 320	-14572 ± 351	-7777 ± 144	994 ± 252	-256 ± 220
Rb	**E1A$_{LxCxE}$**	1.03 ± 0.01	-9522 ± 79	573 ± 92	-8949 ± 47	213 ± 17	
Rb + E1A$_{E2F}$	**E1A$_{LxCxE}$**	1.19 ± 0.01	-8301 ± 89	-565 ± 110	-8867 ± 37	245 ± 27	82 ± 60
Rb + E1A$_{\Delta L}$	**E1A$_{LxCxE}$**	1.13 ± 0.01	-8873 ± 64	78 ± 76	-8795 ± 41	277 ± 20	154 ± 62

All measurements were performed in triplicate except for the Rb-E1A$_{E2F}$, (Rb+E1A$_{LxCxE}$)-E1A$_{E2F}$ and (Rb+E1A$_{LxCxE}$)-E1A$_{\Delta L}$ titrations, which were performed in duplicate.

[1] Titrations with E1A$_{E2F}$ and E1A$_{\Delta L}$ as titrants were performed at 10.0 °C and titrations with E1A$_{LxCxE}$ as titrant, were performed at 20.0 °C.

[2] n values are the average of all independent experimental determinations and the standard deviation is obtained as the propagated mean standard error.

[3] $\Delta\Delta G$ was calculated as $\Delta\Delta G = \Delta G$ pre-saturated - ΔG non-saturated with the complementary motif (or region) to the titrant.

The ΔH and K_D values reported are the average of all independent experimental determinations. The standard deviations for ΔH and K_D are obtained as propagated mean standard errors. ΔG is calculated as $\Delta G = RT*LnK_D$ and $-T\Delta S$ as $-T\Delta S = \Delta G - \Delta H$. The standard deviations for ΔG and $-T\Delta S$ are obtained as the propagated mean standard errors.

Values for thermodynamic parameters are: R = 1.985 cal/K*mol. T = 283.15 K (10 ºC) or T = 293.15 K (20 ºC).

SUPPLEMENTARY FIGURES

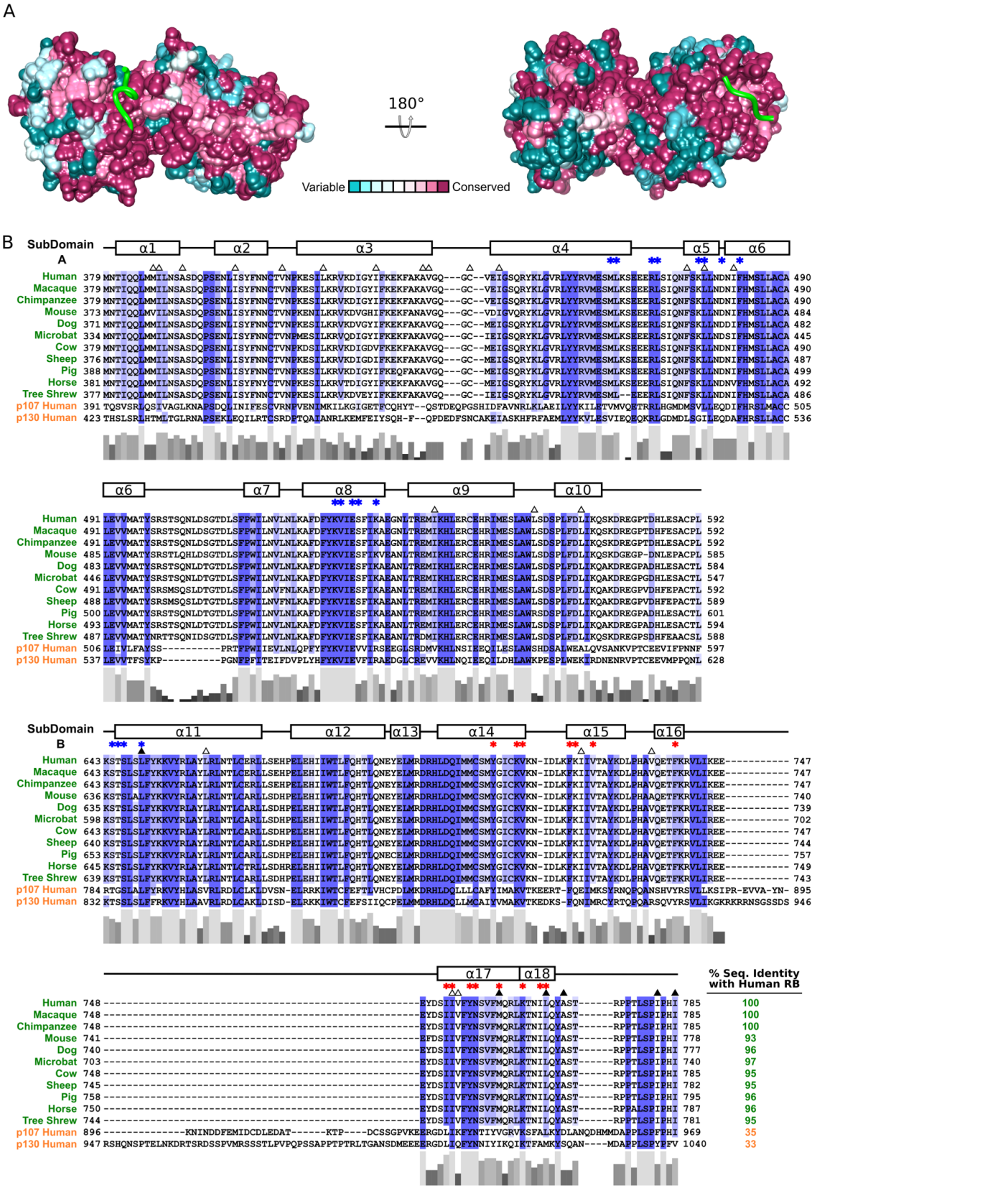

SUPPLEMENTARY FIGURE 1. Sequence conservation across mammalian pocket proteins. a) Evolutionary conservation scores for the Rb pocket domain were calculated with Consurf [16] using an alignment of Rb pocket domain sequences from 77 mammalian species (See Methods). Two views showing the E2F motif binding cleft bound to the E1A E2F motif (PDB: 2R7G) or the LxCxE cleft bound to the E7 LxCxE motif (PDB: 1GUX) are depicted. The color scale indicates the residue conservation score from dark pink (conserved residues) to light blue (variable residues). **b)** Alignment of 11 representative Rb pocket domain sequences from mammalian organisms and human p107/p130. Sequences were aligned using MUSCLE and manually curated. Secondary structure is shown as boxes and positions that contact the E2F (blue stars) and LxCxE (red stars) motifs are indicated at the top of the alignment. Conservation scores are indicated at the bottom [17]. All positions forming the binding sites for the E2F and LxCxE motifs show 100% conservation. Most positions are either strictly conserved or show conservative substitutions in the p107/p130 proteins. Identical residues within columns with a conservation score greater than 50% are colored blue, with darker blue tones indicating a higher degree of conservation.

Supplementary Text 1. Correlation between sequence features of natural E1A linkers and linker dimensions. The correlation between fraction of charged residues (FCR) and linker length reflects the fact that the region used to titrate chain length (Variable region in the linker) is largely depleted of charged residues, such that longer chains have a lower fraction of charged residues. This is an important corollary to the correlation with NCPR, as it demonstrates the neutralization of NCPR is not simply via an increase in the fraction of positive residues, but a relative dilution of charged residues. The negatively charged acidic extensions may generate electrostatic repulsion that ensures the linker stays extended, exposing the associated TAZ2 and MYND motifs, while favoring local solvation that prevents linker-Rb interactions. The negative correlation between normalized end-to-end distance vs. proline content (IV, upper panel) may seem counterintuitive and it implies that less extended chains have a higher proline content. This reflects the fact that the variable region is enriched for proline residues – presumably to prevent local folding – such that as the chain gets longer more proline residues are incorporated. The corollary of the latter explanation suggests that there should be a loss of fractional secondary structure as normalized chain length increases, a result borne out when fractional helicity is compared to normalized end-to-end distance (VI, upper panel). The fraction of helicity is generally between 7% and 1%, suggesting that despite this correlation the effect size is relatively small. As a general conclusion, longer chains become overall more proline rich, hydrophobic, and less highly charged, leading to a relative compensation in their absolute dimensions. This suggests that multiple mechanisms might contribute to fine-tune the dimensions of E1A linkers.

References:

1. Ferreon AC, Ferreon JC, Wright PE, Deniz AA. Modulation of allostery by protein intrinsic disorder. *Nature*. 2013;498(7454):390-394. doi:10.1038/nature12294
2. Uversky VN. What does it mean to be natively unfolded? *Eur J Biochem*. 2002;269(1):2-12. http://www.ncbi.nlm.nih.gov/pubmed/11784292
3. Sherry KP, Das RK, Pappu R V, Barrick D. Control of transcriptional activity by design of charge patterning in the intrinsically disordered RAM region of the Notch receptor. *Proc Natl Acad Sci U S A*. 2017;114(44):E9243-E9252. doi:10.1073/pnas.1706083114
4. Hofmann H, Soranno A, Borgia A, Gast K, Nettels D, Schuler B. Polymer scaling laws of unfolded and intrinsically disordered proteins quantified with single-molecule spectroscopy. *Proc Natl Acad Sci U S A*. 2012;109(40):16155-16160. doi:10.1073/pnas.1207719109
5. Marsh JA, Forman-Kay JD. Sequence determinants of compaction in intrinsically disordered proteins. *Biophys J*. 2010;98(10):2383-2390. doi:10.1016/j.bpj.2010.02.006
6. Perozzo R, Folkers G, Scapozza L. Thermodynamics of protein-ligand interactions: history, presence, and future aspects. *J Recept Signal Transduct Res*. 2004;24(1-2):1-52. http://www.ncbi.nlm.nih.gov/pubmed/15344878
7. Sahu D, Bastidas M, Lawrence CW, Noid WG, Showalter SA. Assessing Coupled Protein Folding and Binding Through Temperature-Dependent Isothermal Titration Calorimetry. *Methods Enzym*. 2016;567:23-45. doi:10.1016/bs.mie.2015.07.032
8. Baldwin RL. Temperature dependence of the hydrophobic interaction in protein folding. *Proc Natl*

Acad Sci U S A. 1986;83(21):8069-8072. http://www.ncbi.nlm.nih.gov/pubmed/3464944
9. Theisen FF, Staby L, Tidemand FG, et al. Quantification of Conformational Entropy Unravels Effect of Disordered Flanking Region in Coupled Folding and Binding. *J Am Chem Soc*. 2021;143(36):14540-14550. doi:10.1021/jacs.1c04214
10. Murphy KP, Freire E. Thermodynamics of structural stability and cooperative folding behavior in proteins. *Adv Protein Chem*. 1992;43:313-361. doi:10.1016/s0065-3233(08)60556-2
11. Myers JK, Pace CN, Scholtz JM. Denaturant m values and heat capacity changes: relation to changes in accessible surface areas of protein unfolding. *Protein Sci*. 1995;4(10):2138-2148. doi:10.1002/pro.5560041020
12. Makhatadze GI, Privalov PL. Energetics of protein structure. *Adv Protein Chem*. 1995;47:307-425. doi:10.1016/s0065-3233(08)60548-3
13. Robertson AD, Murphy KP. Protein Structure and the Energetics of Protein Stability. *Chem Rev*. 1997;97(5):1251-1268. doi:10.1021/cr960383c
14. Spolar RS, Record Jr. MT. Coupling of local folding to site-specific binding of proteins to DNA. *Science (80-)*. 1994;263(5148):777-784. http://www.ncbi.nlm.nih.gov/pubmed/8303294
15. Liu X, Marmorstein R. Structure of the retinoblastoma protein bound to adenovirus E1A reveals the molecular basis for viral oncoprotein inactivation of a tumor suppressor. *Genes Dev*. 2007;21(21):2711-2716. doi:10.1101/gad.1590607
16. Ashkenazy H, Abadi S, Martz E, et al. ConSurf 2016: an improved methodology to estimate and visualize evolutionary conservation in macromolecules. *Nucleic Acids Res*. 2016;44(W1):W344-50. doi:10.1093/nar/gkw408
17. Livingstone CD, Barton GJ. Protein sequence alignments: a strategy for the hierarchical analysis of residue conservation. *Comput Appl Biosci*. 1993;9(6):745-756. doi:10.1093/bioinformatics/9.6.745